HHS Public Access

Author manuscript

J Comp Neurol. Author manuscript; available in PMC 2018 March 01.

Published in final edited form as:

J Comp Neurol. 2017 March 01; 525(4): 850–867. doi:10.1002/cne.24101.

Membrane-Associated Guanylate Kinase scaffolds organize a horizontal cell synaptic complex restricted to invaginating contacts with photoreceptors

Alejandro Vila[1,2], **Christopher M. Whitaker**[1], and **John O'Brien**[*,1,2]

[1]Richard S. Ruiz M.D. Department of Ophthalmology and Visual Science, University of Texas Health Science Center at Houston, Houston, TX, USA

[2]University of Texas Graduate School of Biomedical Sciences at Houston

Abstract

Synaptic processes and plasticity of synapses are mediated by large suites of proteins. In most cases, many of these proteins are tethered together by synaptic scaffold proteins. Scaffold proteins have a large number and typically a variety of protein interaction domains that allow many different proteins to be assembled into functional complexes. As each scaffold protein has a different set of protein interaction domains and a unique set of interacting partners, the presence of synaptic scaffolds can provide insight into the molecular mechanisms that regulate synaptic processes. In studies of rabbit retina, we found SAP102 and Chapsyn110 selectively localized in the tips of B-type horizontal cell processes where they contact cone and rod photoreceptors. We further identified some known SAP102 binding partners, kainate receptor GluR6/7 and inward rectifier potassium channel Kir2.1, closely associated with SAP102 in photoreceptor invaginations. The kainate receptor occupies a position distinct from that of the majority of AMPA receptors that dominate the horizontal cell post-synaptic response. GluR6/7 and Kir2.1 presumably are involved in synaptic processes that govern cell-to-cell communication, and could both contribute in different ways to synaptic currents that mediate feedback signaling. Notably, we failed to find evidence for the presence of Cx57 or Cx59 that might be involved in ephaptic feedback signaling in this complex. The presence of SAP102 and its binding partners in both cone and rod invaginating synapses suggests that whatever mechanism is supported by this protein complex is present in both types of photoreceptors.

Graphical abstract

[*]To whom correspondence should be addressed: 6431 Fannin St., MSB 7.024 Houston, TX 77030, USA John.OBrien@uth.tmc.edu (713) 500-5983.

Conflicts of Interest

All authors declare no conflicts of interest.

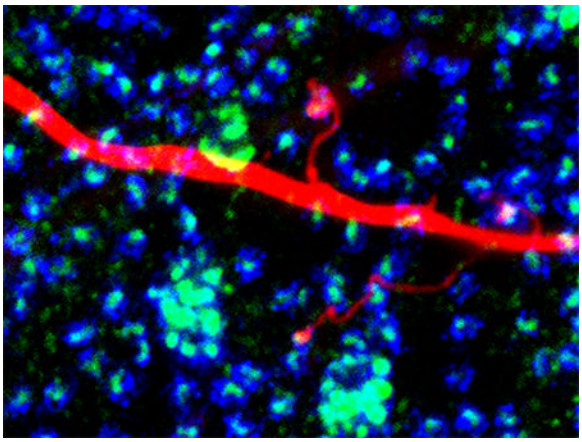

The synaptic scaffold SAP102 is precisely localized in tips of rabbit B-type horizontal cell dendritic and axon terminal (shown) processes where they contact photoreceptors. Specific ion channels including kainate receptor GluR6/7 and inward rectifier potassium channel Kir2.1 are anchored there and may be involved in synaptic feedforward and feedback signaling.

Keywords

Dlg3; Dlg2; Kcnj2; Grik2; synaptic signaling; proximity ligation assay; RRID AB_2261666; RRID AB_2292909; RRID AB_444362; RRID AB_2091920; RRID AB_2277296; RRID AB_2315280; RRID AB_2315430; RRID AB_2314792; RRID AB_641048; RRID AB_1587072; RRID AB_91818; RRID AB_2533518; RRID AB_2314266

INTRODUCTION

The richness of our visual world, with light intensity varying by orders of magnitude and important features demarcated by subtle contrast boundaries, presents challenges to the retinal neurons that code its information. At the first synapse in the visual pathway, the triad synapse between photoreceptors, bipolar cells and horizontal cells (HC), HCs impose inhibitory surround receptive fields that emphasize important information content by subtracting out average light intensity information and enhancing weak contrast features (reviewed by Burkhardt, 1993; Kamermans and Spekreijse, 1999; Thoreson and Mangel, 2012). HCs modulate photoreceptor output through both negative and positive feedback mechanisms. The mechanisms of HC feedback remain controversial, with hypotheses ranging from conventional transmitters (GABA) to non-conventional transmitters (protons) and an ephaptic mechanism (Murakami et al., 1982; Kamermans et al., 2001; Hirasawa and Kaneko, 2003; Vessey et al., 2005; Klaassen et al., 2012). Evidence for each of these mechanisms has been presented in the past decade. All of the feedback mechanisms require precise localization of synaptic events in horizontal cell processes very closely apposed to photoreceptor transmitter release sites.

It is a general rule that precise physical localization of synaptic proteins is essential for effective synaptic transmission and for control of the signaling pathways that impose plasticity. At most synapses, suites of scaffold proteins form complex networks that anchor

receptors and play an important role in synaptic plasticity. Membrane-associated guanylate kinase (MAGUK) proteins are responsible for anchoring many of the necessary components that regulate synaptic transmission (Oliva et al., 2012; Chen et al., 2015). It is well known that excitatory synapses are rich in MAGUKs, including postsynaptic density protein 95 (PSD95 or Dlg4), PSD93 (Chapsyn110 or Dlg2), synapse-associated protein 102 (SAP102 or Dlg3) and synapse-associated protein 97 (SAP97 or Dlg1) (Koulen, 1999). These synaptic scaffolding proteins share homologous PDZ, MAGUK, and SH3 domains, which mediate protein-protein interactions to form multi-protein complexes. The complexes of synaptic scaffolds often include a variety of transmitter receptors, ion channels, and regulatory proteins.

To provide insight into HC synaptic mechanisms, we sought to identify neuronal scaffold proteins that reside in the synapse between photoreceptors and HCs. We systematically evaluated the distributions of several synaptic scaffold proteins in rabbit retina, finding scaffolds restricted to the tips of horizontal cells contacting photoreceptors, and further examined the localization of proteins known to interact with them. We find evidence that scaffolds assemble a complex of proteins that are likely involved in synaptic signaling between photoreceptors and horizontal cells.

MATERIALS AND METHODS

Tissue preparation

Retinas from New Zealand White rabbits ranging between 3–5 kg of weight were used in this study. These animals were anesthetized with a mixture of ketamine/xylazine (40/5 mg/kg) by IM injection and euthanized with an overdose of sodium pentobarbital (100 mg/kg) following protocols approved by the Institutional Animal Care and Use Committee and conforming to National Institutes of Health (NIH) guidelines. The eyes were enucleated and the anterior segment removed along the ora serrata, followed by removal of vitreous humor. The resulting retina-sclera preparation was cut into 4 to 5 sections and the tissue pieces maintained in carboxygenated Ames' medium (Sigma-Aldrich, St. Louis, MO) at ambient temperature. For light microscopy, tissue pieces were immersion fixed in either 4% (w/v) paraformaldehyde (PFA) or 4% N-(3-dimethylaminopropyl)-N′-ethylcarbodiimide hydrochloride (EDAC; Sigma-Aldrich) in 0.1M phosphate buffer (PB; pH 7.4). We found 20 minutes in 4% EDAC fixation was the best condition to visualize synaptic proteins. Retinal pieces were cryoprotected in 30% sucrose in PB overnight at 4°C, sectioned vertically at 12μm on a cryostat and collected on slides. For whole mount preparations, retinas were isolated from eyecup, flattened on a black nitrocellulose filter paper (Millipore, Billerica, MA) and fixed in 4% EDAC for 1 hour to preserve tissue integrity.

Injection of Neurobiotin and Alexa 568

Retinas were isolated from the eyecup while immersed in carboxygenated (95% O_2 + 5% CO_2) Ames medium (US Biological, Swampscott, MA) and mounted on 0.8μm black filter paper (Millipore, Bedford, MA). Retinal cells were prelabeled with 5μM 4,6-diamino-2-phenylindole (DAPI) (Invitrogen, Carlsbad, CA) in Ames medium for 15 minutes. Retinal pieces prelabeled with DAPI were visualized on an Olympus BX-50WI microscope (Tokyo,

Japan) equipped with epifluorescence. Targeted horizontal cells were impaled under visual control with 150–200 MΩ glass electrodes (Warner Instruments, Hamden, CT) pulled on a horizontal electrode puller (Sutter Instruments, Novato, CA). Electrodes tips were filled with 4% Neurobiotin (Vector Laboratories, Burlingame, CA) and 0.5% Lucifer Yellow-NH_4 (Molecular Probes, Eugene, OR) in 0.05M PB, then backfilled with 3M LiCl. Electrodes tip-filled with Alexa 568 (Molecular Probes; A10437) were back-filled with 3M KCl. Impaled cells were injected with a biphasic current (±2.0 nA, 3Hz) for 4–5 mins. Following the last injection, retinal pieces were fixed in 4% PFA for 30 minutes prior to further immunohistochemical processing. For single cell injections, 50μM meclofenamic acid was perfused over the retina for 15 min prior to Neurobiotin injection.

Immunolabeling

Retinal sections were labeled with antiserum in tissue treated with 0.3% Triton X-100 (Sigma-Aldrich) and incubated overnight with 3% Donkey Serum in Dulbecco's Phosphate Buffered Saline (PBSA) at room temperature (RT) to block non-specific immunolabeling. For flat mount preparations, retinal pieces were incubated for a minimum of 5 days in a rotator at 4°C. Antibodies used included mouse IgG_1 anti-SAP-102 clone N19/2 (1:500; UC Davis/NIH NeuroMab Facility, Davis, CA), mouse IgG_1 anti-SAP97 clone K64/15 (1:500, UC Davis/NIH NeuroMab Facility, Davis, CA), mouse IgG_1 anti-Chapsyn-110 clone N18/30 (1:500; UC Davis/NIH NeuroMab Facility, Davis, CA) and mouse IgG_{2a} anti-PSD95 clone K28/43 (1:500; UC Davis/NIH NeuroMab Facility, Davis, CA). The tissue was rinsed in PBSA extensively and double- or triple-labeled with either goat IgG anti-GluR5 C-18 (1:500, Santa Cruz Biotechnology, Santa Cruz, CA) or rabbit antibodies including anti-mGluR6, against the C-terminal peptide (KATSTVAAPPKGEDAEAHK) of human metabotropic glutamate receptor 6 (1:500; gift of Dr. Noga Vardi; (Vardi et al., 2000)), anti-GluR6/7 clone NL9 (1:500, Millipore), and anti-Kir2.1 (1:200, Millipore). Additional information about the antibodies is given in Table 1. Most secondary antibodies were raised in donkeys and affinity purified. These included Alexa Fluor 488 and/or Cy3 anti-goat IgG (1:1,000; Jackson Immunoresearch, West Grove, PA), Alexa 488 and/or Cy3 anti-rabbit IgG (1:500; Molecular Probes, Eugene, OR) and Dyelight 647 anti-mouse IgG (1:500; Jackson Immunoresearch). Additionally, anti-mouse IgG subtype specific secondary antibodies raised in goats were used at times to double label with two mouse monoclonals. These included Alexa 488 anti-mouse IgG_1 and Cy3 anti-mouse IgG_{2a} (1:500; Jackson Immunoresearch). Sections were incubated in secondary antibodies for 1 hour at room temperature, and pieces of retina were left in secondary antibody for 1 day at 4°C. Tissue was coverslipped in Vectashield mounting medium (Vector Laboratories, Burlingame, CA) with DAPI.

Several additional antibodies were used as markers for specific cell types or for synaptic structures. Affinity-purified anti-syntaxin 3 specific antibody generated in rabbits against a peptide from the N-terminus of mouse syntaxin 3 KDRLEQLKAKQLTQDDC (1:100; gift of Dr. Roger Janz); anti-ribeye, U2656, raised in rabbits against a purified glutathione S-transferase (GST) fusion protein containing the entire B domain of rat ribeye (1:500; gift of Dr. Thomas Südhof; (Schmitz et al., 2000); anti-Cx57 raised in rabbits against a mouse Cx57 C-terminal peptide, aa434–446 (1:100; Invitrogen); anti-Cx59, raised in rabbits against

a C-terminal peptide of the human Cx59, aa486–501 (1:100; gift of Dr. Steve Massey); anti-Pannexin 2 raised in rabbits against a peptide corresponding to the C-terminus of mouse Panx2 (1:200; TermoFisher, Waltham, MA).

In situ Proximity Ligation Assay (PLA)

Potential protein-protein interactions were assessed by in situ Proximity Ligation Assays (PLA). PLA was performed using a generalized Duolink mouse/rabbit labeling kit (Olink Bioscience, Uppsala, Sweden). To optimize results we fixed retinas with 4% EDAC in 0.1M PB for 30 minutes at room temperature followed by 4% PFA for 5 minutes. This fixation protocol worked well and was used for studying SAP102 interactions with either GluR6/7 or Kir2.1. We used conventional immunohistochemistry techniques for labeling retinal cryostat sections with mouse and rabbit primary antibodies. Briefly, retinal sections were blocked with 15% normal donkey serum in 0.1M PB with 0.3% TritonX-100 detergent and then incubated with primary antibodies in the same solution overnight at 4°C. On the following day, sections were washed three times with 0.1M PB for 10 min each with gentle shaking. After primary incubation, all further steps were done according to the Duolink manual. Incubations with the kit-derived oligonucleotide-linked secondary antibodies, PLA probe dilution/incubation time, ligation, rolling circle amplification times and polymerase concentrations were optimized for retinal sections (Leuchowius et al., 2011). PLA probes were incubated in pre-heated humidity chamber for 60 min at 37°C, briefly washed three times and left with gentle shaking for 30 min in Duolink buffer A. The slides were further processed for ligation for 60 min at 37°C, and amplification step was significantly improved when incubation time was 60min at 37°C.

To verify the selectivity of the PLA experiments, we used the antibodies mouse anti-SAP102 (cat# 75-058, UC Davis/NIH Neuromab Facility), rabbit anti-GluR6/7 (cat#04–921, Millipore Corporation), rabbit anti-Syntaxin 3 (gift or Dr. Roger Janz) and rabbit anti-PSD95 (cat#18258, Abcam, Cambridge, MA). We performed negative controls by excluding one of the probes during antibody incubation or by probing for proteins known to be on opposite sides of the synapse (e.g. SAP102 and syntaxin 3). We performed positive controls by probing with two different antibodies to the same protein (not shown).

Confocal microscopy

Image acquisition was performed with a Zeiss LSM 510 META laser scanning confocal microscope (Carl Zeiss, Thornwood, NY). All sections were imaged with dye-appropriate filters (405 nm excitation, 440–460 nm emission for DAPI; 542 nm excitation, 590–620 nm emission for Cyanine 3; 488 nm excitation, 530–550 nm emission for Alexa 488; 633 nm excitation, long-pass 650 nm emission for Dyelight 647). The detector gain and offset parameters were adjusted so that the intensity of most pixels fell within the dynamic range of the detector and the intensity of the most brightly labeled immunoreactive puncta showed very limited saturation. Images were acquired with a 40× or 63× oil-immersion objectives as a series of optical sections ranging between 0.25 to 0.5 μm in step size. Each marker was assigned a pseudocolor and the images were analyzed as single optical sections and as stacks of optical sections projected along the y or z axis. All images were processed in Adobe Photoshop (Adobe Systems CS5, San Jose, CA) to enhance brightness and contrast.

Antibody characterization

Antibodies used in this study have been characterized previously using western blots and/or immunohistochemistry. Summary characterization data are included below; see table 1 for additional antibody information.

The SAP102 monoclonal antibody (UC Davis NeuroMab cat. no. 75-058; RRID: AB_2261666) recognized a single band of 105 KDa in western blots of rat and mouse brain membranes (UC Davis/NIH NeuroMab Facility, Davis, CA). SAP102 labeling was previously examined in rat and monkey retina; it was found in horizontal cell processes contacting photoreceptor terminals (Koulen et al., 1998b; Haverkamp et al., 2000).

The PSD95 monoclonal antibody (UC Davis NeuroMab cat. no. 75-028; RRID: AB_2292909) blotted against mouse and rat brain homogenates recognized multiple bands 95–110 kDa due to changes in background phosphorylation (UC Davis/NIH NeuroMab Facility, Davis, CA). This antibody labeled proteins encircling the plasma membranes of photoreceptor terminals in the OPL (Li et al., 2013; Puthussery et al., 2014).

The SAP97 monoclonal antibody (UC Davis NeuroMab cat. no. 75-030; RRID: AB_2091920) recognized a single band of 130 KDa on western blots of mouse and rat brain (UC Davis/NIH NeuroMab Facility, Davis, CA). It reproduced the pattern of labeling described previously in rat retina; that is, photoreceptor terminals in the OPL (Koulen, 1999).

The Chapsyn110 monoclonal antibody (UC Davis NeuroMab cat. no. 75-057; RRID: AB_2277296) blotted against crude membranes from human brain recognized a single band of 110KDa. Multiple bands were observed in immunoblots against crude membranes from whole adult mouse and rat brains (UC Davis/NIH NeuroMab Facility, Davis, CA). Immunoreactivity for this antibody had strong punctate distribution in both the OPL and IPL, as previously described (Koulen, 1999).

The ribeye antiserum (RRID: AB_2315280) recognized only two bands on western blots of bovine retina: one at 120 kDa corresponding to the predicted molecular weight of ribeye and one at 50 kDa corresponding to the predicted molecular weight of CtBP2, which has a structure identical to that of the B domain of ribeye (Schmitz et al., 2000). Antiserum against ribeye showed a pattern of labeling identical to that observed in other mammalian retinas: it labeled synaptic ribbons in both the outer and inner plexiform layers (Katsumata et al., 2009; Lin et al., 2009).

The syntaxin 3 antibody (RRID: AB_2315430) recognized a single band of 37 kDa in western blots of mouse retina (R. Janz, pers. commun.). The pattern of labeling observed was identical to that described previously in mouse retina: synaptic terminals of photoreceptors and bipolar cells were labeled (Sherry et al., 2006).

The mGluR6 antibody (RRID: AB_2314792) recognized a single band of 190 kDa in western blots of monkey retina (Vardi et al., 2000). It reproduced the pattern of labeling described previously in macaque retina: it labeled the tips of macaque ON bipolar cell dendrites (Gastinger et al., 2006).

The GluR5 affinity-purified goat polyclonal antibodies (Santa Cruz cat. no. sc-7616; RRID: AB_641048) raised against the synthetic peptides comprising the amino acid sequence 900–918 at the C-terminus and the amino acid sequence 1–20 at the N-terminus of GluR5 of human origin have been shown previously to label OFF cone bipolar dendrites in rabbit retina (Pan and Massey, 2007).

The GluR6/7 antibody (Millipore cat. no. 04–921; RRID: AB_1587072) recognized a single band of 115 KDa in western blots of mouse brain preparations (Darstein et al., 2003). This antibody labeled HC dendrites invaginating in photoreceptor terminals, as previously described (Peng et al., 1995). The pattern of labeling was localized in the outer portion of the OPL, where GluR6/7 was expressed at the cone pedicles of the primate (Haverkamp et al., 2001a).

The Kir2.1 affinity purified polyclonal antibody (Millipore cat. no. AB5374; RRID: AB_91818) recognized a single band of 48 KDa corresponding to the predicted molecular weight of Kir2.1 (Giovannardi et al., 2002). Kir2.1 is highly expressed in the superior colliculus (Pruss et al., 2005), however its distribution is yet to be reported in the retina.

Pannexin 2 affinity-purified rabbit polyclonal antibody (ThermoFisher cat. no. 42–2800; RRID: AB_2533518) was raised against a synthetic peptide derived from the C-terminal region of mouse and rat pannexin 2, which differs by one non-conservative amino acid replacement from human and from predicted monkey, bovine, and dog proteins. On Western blots, it identifies the target band at 103 kDa in pannexin 2-GFP-transfected C6 cells (Lai et al, 2009). Pannexin 2 is abundantly expressed in the CNS (Bruzzone et al., 2003).

Rabbit anti-Cx57 (C-term) polyclonal antibody (Invitrogen cat. no. 40–4800; RRID: AB_2314266) was raised against mouse (rat) connexin 57 (C-term) (aa 434–446) (Ciolofan et al., 2007). Anti-connexin 57 (C-term) recognizes the expressed product of the Gja10 gene. On western blots it identifies bands at ≈54 kDa (Cx57) as well as other unidentified bands. This antibody produced punctate labeling of Cx57 in the OPL of the mouse retina. Unfortunately, this labeling pattern was also present in the Cx57 knockout mouse (Ciolofan et al., 2007).

Rabbit anti-Cx59 (C-term) is a polyclonal antibody raised against a synthetic peptide comprising the amino acid sequence 486 −501 at the C-terminus of human Cx59, which differs by one non-conservative amino acid replacement from rabbit protein. Anti-connexin 59 (C-term) recognizes the expressed product of the GJA9 gene. Cx59 is not found in the mouse genome (Sohl and Willecke, 2003). Cx59 is related to zebrafish Cx55.5 and was reportedly detected as a transcript in the human retina (Sohl et al., 2010); no reports of immunostaining for this connexin have been published. Cx59 antibody labeled small puncta in the OPL of the rabbit retina when fixed with EDAC; no labeling was present in formaldehyde-fixed retina.

RESULTS

Distribution of MAGUK-containing synaptic scaffold proteins in the retina

Synaptic scaffold proteins bind to and assemble unique suites of proteins that establish the functional properties of synapses. Because each scaffold may assemble different groups of proteins, certain aspects of the functional properties of a synapse can be inferred from the scaffolds that are present. To gain insight into the synaptic interactions of retinal photoreceptors, we examined the distribution of the MAGUK-containing synaptic scaffold proteins in the rabbit outer plexiform layer (OPL) by multiple-label immunofluorescence and confocal microscopy. Labeling for PSD95 followed its well-known but paradoxical labeling pattern as a pre-synaptic marker encircling the plasma membranes of both rod and cone terminals (Fig. 1A). SAP97 gave a similar labeling pattern (Fig. 1B). Both SAP97 and PSD95 were also present in the inner plexiform layer (IPL), although PSD95 labeling was very weak. In contrast to the distribution of these proteins, immunoreactivity for SAP102 (Fig. 1C) had a strong punctate distribution in both the OPL and the IPL. The distribution of Chapsyn110 was similarly punctate in the OPL (Fig. 1D) and quite abundant and punctate in the IPL.

SAP102 is a postsynaptic element of photoreceptor synapses

The punctate distribution of SAP102 and Chapsyn110 that did not show the outline of photoreceptor terminals suggested that these scaffolds might be post-synaptic in the OPL. To assess their distribution, we first examined the localization of SAP102 in more detail. In whole mount views of the OPL, SAP102 immunoreactivity appeared as tight clusters of round puncta surrounded by smaller, sparser puncta (Fig. 2A). Labeling with an antibody to GluR5, a kainate receptor in OFF bipolar cell dendrites at the base of cone pedicles (Haverkamp et al., 2003), revealed that the tight clusters of SAP102 labeling were located at cone pedicles (Fig. 2A). In vertical sections SAP102-immunoreactive (IR) puncta were located slightly above GluR5 labeling (Fig. 2B), a finding suggesting that SAP102 was located inside cone pedicles. Chapsyn-110 had a similar distribution with clusters of puncta associated with cones and distributed individual puncta in the OPL (Fig. 2C).

To determine whether SAP102 was localized to photoreceptor terminals, retinas were double-labeled with antibodies to syntaxin 3, a membrane protein expressed by rods and cones that is a component of the soluble N-ethylmaleimide-sensitive factor attachment protein receptor (SNARE) complex at ribbon synapses (Morgans et al., 1996). Immunolabeling of syntaxin 3 is found in the membranes of cone and rod photoreceptor synaptic terminals (Li et al., 2009; Vila et al., 2012). Strong syntaxin 3 immunolabeling was found at the plasma membrane of synaptic terminals in rods (Fig. 3A). In cone terminals, however, a small amount of diffuse cellular staining was present. Single optical sections through the OPL double labeled with SAP102 and syntaxin 3 antibodies showed punctate staining closely associated with each other but the two were not colocalized (Fig. 3B). SAP102 puncta in the form of clusters were localized slightly above the plasma membrane (Fig. 3C), suggesting that SAP102 is inside of cone pedicles and not in their plasma membrane. One punctum was typically found in the center of each rod spherule (Fig. 3B).

Similar to the situation in cones, the SAP102 label was found in a gap in syntaxin 3 labeling, suggesting that SAP102 was present in a process invaginating the rod spherule.

Double labeling using an antibody to the synaptic ribbon protein ribeye revealed that SAP102 was closely associated with photoreceptor synaptic ribbons, but ribeye and SAP102 were not colocalized (Fig. 3D). SAP102 immunoreactivity was always localized below the cone and rod synaptic ribbons, suggesting that it is post-synaptic to the photoreceptors, but localized well within the invaginating synapses of the photoreceptors. Two cell types have processes post-synaptic to photoreceptors within the invaginating synapses: ON (depolarizing) bipolar cells and horizontal cells. To determine whether SAP102 was associated with ON bipolar cell dendrites, we performed double labeling studies using an antibody to the ON bipolar cell glutamate receptor mGluR6 (Fig. 3E). ON bipolar cell dendrites were also closely associated with SAP102-IR puncta, but the two were not colocalized. The SAP102-IR puncta were always located above ON bipolar cell dendrites (Fig. 3F).

SAP102 is located in B-type horizontal cells

The lack of co-localization of SAP102 immunoreactivity with either ON or OFF bipolar cell markers and its apparent post-synaptic localization suggests that it may be located in horizontal cells. In the rabbit, A-type horizontal cells (HCs) send dendritic processes only into the invaginating synapses in cone pedicles, while B-type HCs send dendritic processes to cone pedicles and axon terminal processes to rod spherules. To examine whether SAP102 was expressed by horizontal cell dendrites, the lateral elements of the triads, cell bodies of HCs were visualized with DAPI and injected with Neurobiotin using intracellular electrodes. Horizontal cells of both types form extensively overlapping matrices, with a coverage factor of about 6 for A-type HCs and 8 to 10 for B-type HCs (Mills and Massey, 1994), and extensive gap junctional coupling that permits diffusion of tracers. In order to visualize single cells well, we incubated the retinas with meclofenamic acid to inhibit gap junction coupling prior to injections (see Methods). Injection of A-type HCs and double labeling with anti-SAP102 revealed that the tips of A-type HC processes were closely associated with SAP102 clusters, but the two markers failed to colocalize (Fig. 4A–D).

In contrast to the results with A-type HCs, double-labeling experiments with Neurobiotin-filled B-type HCs and SAP102 antibodies showed dendritic processes colocalized with SAP102 (Fig. 4E–H). Dendrites of B-type horizontal cells sent one or more processes to clusters of SAP102 puncta located at cone terminals (Fig. 4F) while the axon terminal complex sent fine processes ending with a single contact on a rod (Fig. 4H). Co-localization was complete at the tips of the HC processes, confirming that B-type horizontal cells contain the SAP102 clusters. Pan and Massey (2007) have previously shown that rods in rabbit retina are contacted by a single B-type horizontal cell axon terminal process and that each B-type HC axon terminal process contacts only about 10% of immediately adjacent rods due to the extensive overlap with other HCs. Thus the extension of processes contacting a limited number of rods within the axon terminal field (Fig. 4H) is expected. Likewise, the extension of B-type HC dendritic processes to make a single contact with a cone (Fig. 4F) is also expected. The presence of SAP102 in both cone and rod invaginating synapses suggests that

whatever mechanism is supported by this protein complex is present in both types of photoreceptors. These proteins may be involved in either feedforward or feedback signaling between the photoreceptors and the horizontal cell.

Proteins known to bind to SAP102 are present in HC synapses

To determine whether SAP102 in horizontal cells was associated with some of its known interacting partners, we double- and triple stained specimens with specific antibodies against glutamate receptors and potassium channels. The kainate receptor GluR6 has been found to bind to SAP102 in vitro (Cai et al., 2002) and an antibody against GluR6/7 has previously been found to label processes of horizontal and bipolar cells in mammalian retina (Peng et al., 1995). We found strong GluR6/7 staining distributed in the OPL, where the protein had a punctate appearance with the formation of aggregates adjacent to cone pedicles (Fig. 5A, B). These aggregates colocalized completely with SAP102 at cone pedicles. Higher magnification images showed less pronounced GluR6/7 immunoreactivity in the form of single puncta above the level of cone pedicles, colocalizing with SAP102 (Fig. 5C). In vertical sections (Fig. 5D) GluR6/7 labeling was also clearly colocalized with the clusters of SAP102 associated with the invaginations of rod spherules. The localization of the kainate receptor GluR6/7 was quite different than that of AMPA receptors, which are predominantly localized just outside of the synaptic cleft at desmosome-like junctions below cone pedicles and at comparable locations along the shaft of processes leading to rods (Haverkamp et al., 2001b; Pan and Massey, 2007).

Another protein that has been demonstrated to associate with SAP102 is the inward rectifier potassium channel Kir2.1 (Leonoudakis et al., 2004). Kir2.1 immunolabeling exhibited a mixture of diffuse and punctate patterns in the OPL and surrounded the somas of HCs (Fig. 6A). Labeling for Kir2.1 extended to the outermost part of the OPL and sometimes localized to specific areas close to photoreceptors. To evaluate whether Kir2.1 was present in HCs, we triple-labeled sections with antibodies to Kir2.1, SAP102, and GluR6/7 (Fig. 6B–E). Figure 6B (SAP102 alone) and C (triple label) show one SAP102 cluster at a cone terminal with surrounding rod spherule contacts. The numbers 1, 2 and 3 designate single SAP102 puncta contacting a cone (1) or rods (2 and 3). Figure 6C shows the triple-labeled specimen and the insets 1–3 show enlarged single optical sections of the three single puncta at the level of the cone contacts. Figure 6D and E show the same sample 0.35 μm higher in the OPL, at the level of the rod contacts, and insets 4–6 show the same SAP102 puncta as 1–3. Kir.2.1 immunoreactivity was found directly colocalized with SAP102 puncta at the invaginated tips of both HC dendritic processes contacting cones and axon terminal processes contacting rods in the OPL. Only Kir2.1 puncta were colocalized in the outermost portion of the OPL, suggesting that Kir2.1 was clustered by SAP102 in the tips of HC processes.

Proteins thought to mediate ephaptic feedback signaling were not present in the scaffolded complex

Connexin hemichannels at the tips of HC dendrites have been proposed to function as a current source for ephaptic feedback from HCs to cones (Kamermans et al., 2001). To evaluate whether SAP102 was associated with connexin hemichannels we performed double labeling studies using antibodies against connexin 57 (Cx57) and Cx59. We found Cx57

immunoreactive clusters in the OPL and scattered through the nuclear layers (Fig. 7A). Labeling in the nuclear layers with this antibody has previously been found to be non-specific, while labeling in the OPL detected Cx57 gap junctions (Pan et al., 2012). Cx57 gap junctions in the OPL were located mostly below the SAP102-IR puncta (Fig. 7A), suggesting that Cx57 plaques lie at the bottom of the HC processes. No apparent relationship between the Cx57 plaques and either cone pedicles or rod spherules was observed. Labeling for Cx59 in the OPL similarly showed small puncta that did not have any relationship to the SAP102 clusters associated with cones or rods (Fig. 7B). Thus, neither connexin was associated with SAP102 nor was either detectable at the tips of horizontal cell processes.

Close associations of SAP102 with ion channels in the OPL

The placement of ion channels at the tips of horizontal cell processes deep within the invaginating synapses in cones and rods gives them preferential access to the physical environment of the synapse, which may be particularly important for post-synaptic signaling and feedback signaling from HCs to photoreceptors. We hypothesize that the role of the synaptic scaffold SAP102 is to hold these channels in this location to facilitate synaptic signaling. To assess whether SAP102 is bound to GluR6/7 and Kir2.1 in the OPL, we used in situ proximity ligation assays (PLA). The indirect method we used detects protein proximity up to about 40 nm apart, suggesting that positive signals represent either direct protein-protein interactions or very close association of proteins that could be via indirect interactions. Figure 8 shows SAP102 labeling in a section of rabbit retina (A) and PLA reaction product for interaction between SAP102 and GluR6/7 (B) in a sequential section. While SAP102 immunoreactivity occurred in both the OPL and IPL, the PLA reaction product was restricted to the OPL and appeared punctate. In a similar fashion, the PLA reaction product for interaction between SAP102 and Kir2.1 was restricted to a narrow band of puncta in the OPL (Fig. 8E). This distribution was much more restricted than that of SAP102 immunoreactivity in an adjacent section (Fig. 8D) or the observed distribution of Kir2.1 in the OPL (see Fig. 6A). Figure 8G–I shows a negative control experiment in which an interaction between SAP102 and syntaxin 3 was tested by PLA. Although these proteins occur very close to each other on opposite sides of the photoreceptor synapses, no reaction product was detected in the OPL (Fig. 8H). The results indicate that GluR6/7 and Kir2.1 are very closely associated with SAP102 in the OPL, and thus supports the hypothesis that SAP102 likely interacts with these proteins to form a complex within the tips of HC processes. To our knowledge, this is the first time that interactions between SAP102 and either kainite receptors or potassium channels have been reported by in situ proximity ligation assay (PLA).

DISCUSSION

Chemical synapses are marked by the presence of complex signaling networks associated with synaptic scaffolds. In postsynaptic densities, scaffolds interact with neurotransmitter receptors and many other proteins to organize microdomains that mediate synaptic transmission and influence plasticity (Tomita et al., 2001; Cuthbert et al., 2007; Zheng et al., 2011). Genetic deletion of specific scaffolds results in alterations of synaptic transmission and scaffold-specific deficits in certain cognitive tasks (Cuthbert et al., 2007; Nagura et al.,

2012). Thus, synapses can be organized by different sets of interacting proteins that therefore comprise a unique molecular signature.

In this study, we characterized MAGUKs and their interacting partners associated with processes postsynaptic to photoreceptors, extending previous studies demonstrating the localization of some MAGUKs to photoreceptor synapses (Koulen et al., 1998a; Koulen et al., 1998b). In the present study, we found that SAP102 organized a complex containing GluR6/7 and Kir2.1 in the tips of dendritic and axon terminal processes of B-type horizontal cells where they invaginate cone and rod photoreceptors. Chapsyn110 was also likely a component of this complex. Most previous studies show AMPA-type glutamate receptors to be the predominant form of glutamate receptor in mammalian horizontal cells, with dense clusters localized below cone and rod terminals and only a small fraction localized to the invaginating tips of dendritic or axon terminal processes (Haverkamp et al., 2001b; Pan and Massey, 2007). Targeted knockout of AMPA receptor GluA4 in mouse horizontal cells reveals a very small persistent glutamate receptor current, amounting to just a few percent of the glutamate-induced current in isolated cells, attributable to kainate receptors (Stroh et al., 2013). Thus the kainate receptor GluR6/7 likely serves a very limited but potentially specialized role in horizontal cell signaling. We hypothesize that this role is in feedback of horizontal cells onto cone and rod photoreceptors.

Inhibitory receptive fields can be imposed by feedback of HC onto photoreceptors. The HC feedback provides dynamic gain control for the photoreceptor synapse and enhances contrast between the center of the receptive field and the surround; this contrast makes for better vision. HC feedback is caused by a shift in the activation curve of the Ca^{2+} current of the photoreceptor (Verweij et al., 1996; Kamermans and Fahrenfort, 2004). The mechanisms that cause this change have been controversial for decades, but appear to include a mechanism that regulates the concentration of protons in the synaptic cleft, modulating the level of inhibition of the photoreceptor voltage-gated Ca^{2+} channel, an ephaptic mechanism that modulates the apparent voltage across the photoreceptor synaptic membrane, and potentially a GABA-based mechanism (Thoreson and Mangel, 2012).

A great deal of evidence has accumulated recently in support of proton-mediated feedback mechanisms. Proton concentration increases in the synaptic cleft of cones when HCs are depolarized in response to glutamate, and is reduced when HCs hyperpolarize (Wang et al., 2014), as would be expected for a dynamic feedback mechanism. Strong pH buffering and alkalinization of the extracellular medium enhance photoreceptor Ca^{2+} current and prevent further enhancement caused by surround illumination that hyperpolarizes HCs, indicating that feedback has been blocked (Hirasawa and Kaneko, 2003; Vessey et al., 2005; Cadetti and Thoreson, 2006). Recent studies propose that protons responsible for acidifying the synaptic cleft come from HCs via a Na^+:H^+ exchanger (Warren et al., 2016), but that regulation of extracellular buffering by bicarbonate is responsible for the modulation of pH (Liu et al., 2013; Warren et al., 2016). An alternative hypothesis proposes that changes in phosphate buffering that is developed via ATP release through Pannexin 1 channels and extracellular hydrolysis of ATP is responsible for the change in cleft pH (Vroman et al., 2014).

A series of studies has indicated that proton-mediated feedback of HCs to photoreceptors is dependent on Ca^{2+}-driven vesicular GABA release from HCs (Liu et al., 2013; Hirano et al., 2016). This is proposed to operate through an unconventional signaling pathway in which GABA activates $GABA_A$ autoreceptors on the horizontal cells, opening a channel permeable to both Cl^- and HCO_3^- (Liu et al., 2013). At depolarized potentials, this would result in an inward flux of HCO_3^- and acidification of the extracellular space, while the reverse would occur at more hyperpolarized potentials negative to the HCO_3^- equilibrium potential. The Ca^{2+} driving GABA release was found to derive largely from voltage-gated Ca^{2+} channels, although some feedback could not be blocked with inhibitors of N- or P/Q-type Ca^{2+} channels (Liu et al., 2013). It is possible that direct Ca^{2+} influx through glutamate receptors could contribute to GABA release. Glutamate receptors of horizontal cells in general have been found to be Ca^{2+}-permeable (Molina et al., 2004). Indeed the GluR6 receptor coded by the unedited mRNA has a Ca^{2+}:monovalent cation permeability ratio of 1.2 (Egebjerg and Heinemann, 1993), suggesting that the kainate receptors we have described at the tips of horizontal cell processes could provide a localized Ca^{2+} signal to support GABA release.

Several studies with isolated horizontal cells have examined modulation of extracellular proton fluxes near the HC plasma membrane. These studies have consistently shown a resting flux of protons out of HCs with a reduction or reversal of flux driven by glutamate stimulation (Molina et al., 2004; Kreitzer et al., 2007; Jacoby et al., 2012). In these studies, proton uptake could be attributed at least partially to Ca^{2+}-dependent activation of the plasma membrane Ca^{2+} ATPase, which functions as a Ca^{2+}/H^+ antiporter. While these results seem to be at odds with findings that HC depolarization enhances proton-mediated feedback to photoreceptors, they reveal mechanisms at work in HCs that may not be detected in the synaptically connected network. We suggest that GluR6/7 kainate receptors at the tips of HC processes could contribute a localized Ca^{2+} signal that activates the Ca^{2+} ATPase.

It is important to consider that receptor desensitization may significantly influence the behavior of kainate receptors on horizontal cells. In isolated horizontal cells from *gluA4* knockout mice, kainate receptor currents were almost completely desensitized until potentiated by the addition of the lectin concanavalin A (Stroh et al., 2013). In general kainate receptors desensitize rapidly upon exposure to glutamate, and kainate receptors deep in the invaginated synaptic cleft of photoreceptors might be expected to be substantially desensitized in the continued presence of glutamate at the dark, resting state in the retina. On the other hand, binding of concanavalin A reduces GluR6 desensitization and binding to the scaffold PSD95 speeds recovery from desensitization (Bowie et al., 2003). While neither of these proteins specifically interacts with kainate receptors on HCs, extracellular matrix proteins may have effects similar to lectins and SAP102 or Chapsyn110 binding may have effects similar to PSD95; neither topic has been specifically investigated. Even in the absence of modulators, kainate receptors on the tips of HC processes would be expected to resensitize somewhat during light exposure on the receptive field center, priming the receptors to signal reductions in brightness.

Horizontal cells have also been proposed to feed back to photoreceptors through an ephaptic mechanism (Kamermans et al., 2001). In this scenario, there is no messenger that is

mediating communication between HC and photoreceptor terminal. Rather, it is an electrical effect due to the voltage drop produced by the flow of synaptic current through the extracellular space. Because the synapse is invaginated and the space between the HC dendrites and the photoreceptor is restricted, the extracellular space has a finite non-zero resistance. Current flow through this space produces a voltage drop that influences the potential across the photoreceptor plasma membrane. Thus, the ephaptic signal causes a change in Ca^{2+} channel activity and the rate of neurotransmitter release.

Negative ephaptic feedback to photoreceptors requires that ion channels in the horizontal cell processes remain open when horizontal cells hyperpolarize, leading to higher synaptic current and higher current through the extracellular space. In the simplest sense, glutamate receptor channels should not provide this service in the receptive field center, as illumination would reduce glutamate release and close the channels. Indeed, glutamate receptors in the synaptic invagination would provide a form of positive ephaptic feedback in the receptive field center (Byzov and Shura-Bura, 1986). Glutamate receptors would still contribute to surround-imposed feedback, and would likely contribute during modest light excursions that do not fully prevent glutamate release. Indeed resensitization of kainate receptors discussed above could contribute in the latter situation with enhancement of current through the synaptic cleft.

In proposing the ephaptic feedback hypothesis, Fahrenfort and Kamermans implicated connexin hemichannels at the tips of HC dendrites to provide the current source (Kamermans et al., 2001). This proposal immediately met with resistance (Deans and Paul, 2001; Dmitriev and Mangel, 2006), but a variety of evidence has supported the presence of connexin hemichannels and their role in feedback in various species (Fahrenfort et al., 2009; Klaassen et al., 2012; Sun et al., 2012; Kemmler et al., 2014), and the presence of Pannexin 1 channels is also thought to provide a route for current flow (Prochnow et al., 2009). It is perhaps surprising that we did not find Cx57 or Cx59 associated with SAP102 in the OPL, which would be expected if either of these connexins formed hemichannels that participated in feedback. One caveat of this result is that the Cx59 antibody has not been well characterized, so it is not certain that this negative result is completely reliable. We did not find antibodies to Pannexin 1 that worked in the rabbit retina, so we were not able to assess whether this channel might be involved in feedback.

One significant finding of our study was identification of Kir2.1 as a component of the postsynaptic complex in photoreceptor invaginating synapses. Under physiological conditions, this inward rectifier channel opens upon hyperpolarization, generating a large inward K^+ conductance at potentials negative to E_K (Hibino et al., 2010). Unlike connexin hemichannels or pannexin channels that should be open at the dark resting potential and provide instantaneous ephaptic feedback upon hyperpolarization, Kir2.1 channels would open upon hyperpolarization, developing ephaptic feedback with a time constant dependent on the time constant of channel opening. Horizontal cell feedback develops with a relatively slow time course (Kamermans et al., 2001), which has been attributed to alleviation of proton-mediated Ca^{2+} channel inhibition by dissipation of an ATP-ADP-H^+ buffer in the synaptic cleft (Vroman et al., 2014). The delayed activation time course of Kir2.1 channels

would be more consistent with observed feedback signals, making it a plausible channel for the generation of ephaptic feedback.

Two types of positive feedback have recently been observed at the horizontal cell to photoreceptor synapse. One form is imposed by the surround and enhances the gain of the photoreceptor synapse (VanLeeuwen et al., 2009). This form is a corollary to the negative feedback, resulting from the shift of the voltage dependence of the Ca^{2+} channel activation curve. The other form of positive feedback is local (Jackman et al., 2011). The mechanism of this feedback is not fully elucidated, but it depends on Ca^{2+} rise in the horizontal cell and activation of AMPA-type glutamate receptors. It is unclear if kainate-type glutamate receptors could contribute to this mechanism, but the relatively high Ca^{2+} permeability of GluR6 receptors suggests that these receptors could provide Ca^{2+} to support this mechanism. This remains a possible role for the GluR6/7 receptors we find localized in the tips of horizontal cell processes contacting photoreceptors.

Acknowledgments

Supported by NIH grant EY012857 (JO), core grant EY10608, the Frederic B. Asche endowment (JO), and a challenge grant to the Ruiz Department of Ophthalmology & Visual Science from Research to Prevent Blindness.

Other Acknowledgements

We thank Dr. Roger Janz (University of Texas Health Science Center at Houston) for the gift of syntaxin 3 antibody, Dr. Steve Massey (University of Texas Health Science Center at Houston) for the gift of Cx59 antibody, Dr. Noga Vardi (University of Pennsylvania) for the gift of mGluR6 antibody, and Dr. Thomas Sudhof (Stanford University) for the gift of ribeye antibody.

Roles of Authors

AV designed the project, performed experiments, analyzed data and wrote the paper; CMW performed experiments; JO designed the project, analyzed data and wrote the paper.

LITERATURE CITED

Bowie D, Garcia EP, Marshall J, Traynelis SF, Lange GD. Allosteric regulation and spatial distribution of kainate receptors bound to ancillary proteins. J Physiol. 2003; 547(Pt 2):373–385. [PubMed: 12562952]

Bruzzone R, Hormuzdi SGT, Barbe M, Herb A, Monyer H. Pannexins, a family of gap junction proteins expressed in brain. PNAS. 2003 2233464100.

Burkhardt DA. Synaptic feedback, depolarization, and color opponency in cone photoreceptors. Vis Neurosci. 1993; 10(6):981–989. [PubMed: 8257672]

Byzov AL, Shura-Bura TM. Electrical feedback mechanism in the processing of signals in the outer plexiform layer of the retina. Vision Res. 1986; 26(1):33–44. [PubMed: 3012877]

Cadetti L, Thoreson WB. Feedback effects of horizontal cell membrane potential on cone calcium currents studied with simultaneous recordings. J Neurophysiol. 2006; 95(3):1992–1995. [PubMed: 16371457]

Cai C, Coleman SK, Niemi K, Keinanen K. Selective binding of synapse-associated protein 97 to GluR-A alpha-amino-5-hydroxy-3-methyl-4-isoxazole propionate receptor subunit is determined by a novel sequence motif. J Biol Chem. 2002; 277(35):31484–31490. [PubMed: 12070168]

Chen X, Levy JM, Hou A, Winters C, Azzam R, Sousa AA, Leapman RD, Nicoll RA, Reese TS. PSD-95 family MAGUKs are essential for anchoring AMPA and NMDA receptor complexes at the postsynaptic density. Proc Natl Acad Sci U S A. 2015; 112(50):E6983–E6992. [PubMed: 26604311]

Ciolofan C, Lynn BD, Wellershaus K, Willecke K, Nagy JI. Spatial relationships of connexin36, connexin57 and zonula occludens-1 in the outer plexiform layer of mouse retina. Neuroscience. 2007; 148(2):473–488. [PubMed: 17681699]

Cuthbert PC, Stanford LE, Coba MP, Ainge JA, Fink AE, Opazo P, Delgado JY, Komiyama NH, O'Dell TJ, Grant SG. Synapse-associated protein 102/dlgh3 couples the NMDA receptor to specific plasticity pathways and learning strategies. J Neurosci. 2007; 27(10):2673–2682. [PubMed: 17344405]

Darstein M, Petralia RS, Swanson GT, Wenthold RJ, Heinemann SF. Distribution of kainate receptor subunits at hippocampal mossy fiber synapses. J Neurosci. 2003; 23(22):8013–8019. [PubMed: 12954862]

Deans MR, Paul DL. Mouse horizontal cells do not express connexin26 or connexin36. Cell Adhes Commun. 2001; 8(4–6):361–366.

Dmitriev AV, Mangel SC. Electrical feedback in the cone pedicle: a computational analysis. J Neurophysiol. 2006; 95(3):1419–1427. [PubMed: 16319220]

Egebjerg J, Heinemann SF. Ca2+ permeability of unedited and edited versions of the kainate selective glutamate receptor GluR6. Proc Natl Acad Sci U S A. 1993; 90(2):755–759. [PubMed: 7678465]

Fahrenfort I, Steijaert M, Sjoerdsma T, Vickers E, Ripps H, van Asselt J, Endeman D, Klooster J, Numan R, ten Eikelder H, von Gersdorff H, Kamermans M. Hemichannel-mediated and pH-based feedback from horizontal cells to cones in the vertebrate retina. PLoS One. 2009; 4(6):e6090. [PubMed: 19564917]

Gastinger MJ, Barber AJ, Vardi N, Marshak DW. Histamine receptors in mammalian retinas. J Comp Neurol. 2006; 495(6):658–667. [PubMed: 16506196]

Giovannardi S, Forlani G, Balestrini M, Bossi E, Tonini R, Sturani E, Peres A, Zippel R. Modulation of the inward rectifier potassium channel IRK1 by the Ras signaling pathway. J Biol Chem. 2002; 277(14):12158–12163. [PubMed: 11809752]

Haverkamp S, Ghosh KK, Hirano AA, Wassle H. Immunocytochemical description of five bipolar cell types of the mouse retina. J Comp Neurol. 2003; 455(4):463–476. [PubMed: 12508320]

Haverkamp S, Grunert U, Wassle H. The cone pedicle, a complex synapse in the retina. Neuron. 2000; 27(1):85–95. [PubMed: 10939333]

Haverkamp S, Grunert U, Wassle H. Localization of kainate receptors at the cone pedicles of the primate retina. J Comp Neurol. 2001a; 436(4):471–486. [PubMed: 11447590]

Haverkamp S, Grunert U, Wassle H. The synaptic architecture of AMPA receptors at the cone pedicle of the primate retina. J Neurosci. 2001b; 21(7):2488–2500. [PubMed: 11264323]

Hibino H, Inanobe A, Furutani K, Murakami S, Findlay I, Kurachi Y. Inwardly rectifying potassium channels: their structure, function, and physiological roles. Physiol Rev. 2010; 90(1):291–366. [PubMed: 20086079]

Hirano AA, Liu X, Boulter J, Grove J, Perez de Sevilla Muller L, Barnes S, Brecha NC. Targeted Deletion of Vesicular GABA Transporter from Retinal Horizontal Cells Eliminates Feedback Modulation of Photoreceptor Calcium Channels. eNeuro. 2016; 3(2)

Hirasawa H, Kaneko A. pH changes in the invaginating synaptic cleft mediate feedback from horizontal cells to cone photoreceptors by modulating Ca2+ channels. J Gen Physiol. 2003; 122(6):657–671. [PubMed: 14610018]

Jackman SL, Babai N, Chambers JJ, Thoreson WB, Kramer RH. A positive feedback synapse from retinal horizontal cells to cone photoreceptors. PLoS Biol. 2011; 9(5):e1001057. [PubMed: 21559323]

Jacoby J, Kreitzer MA, Alford S, Qian H, Tchernookova BK, Naylor ER, Malchow RP. Extracellular pH dynamics of retinal horizontal cells examined using electrochemical and fluorometric methods. J Neurophysiol. 2012; 107(3):868–879. [PubMed: 22090459]

Kamermans M, Fahrenfort I. Ephaptic interactions within a chemical synapse: hemichannel-mediated ephaptic inhibition in the retina. Curr Opin Neurobiol. 2004; 14(5):531–541. [PubMed: 15464885]

Kamermans M, Fahrenfort I, Schultz K, Janssen-Bienhold U, Sjoerdsma T, Weiler R. Hemichannel-mediated inhibition in the outer retina. Science. 2001; 292(5519):1178–1180. [PubMed: 11349152]

Kamermans M, Spekreijse H. The feedback pathway from horizontal cells to cones. A mini review with a look ahead. Vision Res. 1999; 39(15):2449–2468. [PubMed: 10396615]

Katsumata O, Ohara N, Tamaki H, Niimura T, Naganuma H, Watanabe M, Sakagami H. IQ-ArfGEF/BRAG1 is associated with synaptic ribbons in the mouse retina. Eur J Neurosci. 2009; 30(8): 1509–1516. [PubMed: 19811534]

Kemmler R, Schultz K, Dedek K, Euler T, Schubert T. Differential regulation of cone calcium signals by different horizontal cell feedback mechanisms in the mouse retina. J Neurosci. 2014; 34(35): 11826–11843. [PubMed: 25164677]

Klaassen LJ, Fahrenfort I, Kamermans M. Connexin hemichannel mediated ephaptic inhibition in the retina. Brain Res. 2012; 1487:25–38. [PubMed: 22796289]

Koulen P. Localization of synapse-associated proteins during postnatal development of the rat retina. Eur J Neurosci. 1999; 11(6):2007–2018. [PubMed: 10336670]

Koulen P, Fletcher EL, Craven SE, Bredt DS, Wassle H. Immunocytochemical localization of the postsynaptic density protein PSD-95 in the mammalian retina. J Neurosci. 1998a; 18(23):10136–10149. [PubMed: 9822767]

Koulen P, Garner CC, Wassle H. Immunocytochemical localization of the synapse-associated protein SAP102 in the rat retina. J Comp Neurol. 1998b; 397(3):326–336. [PubMed: 9674560]

Kreitzer MA, Collis LP, Molina AJ, Smith PJ, Malchow RP. Modulation of extracellular proton fluxes from retinal horizontal cells of the catfish by depolarization and glutamate. J Gen Physiol. 2007; 130(2):169–182. [PubMed: 17664345]

Leonoudakis D, Conti LR, Anderson S, Radeke CM, McGuire LM, Adams ME, Froehner SC, Yates JR 3rd, Vandenberg CA. Protein trafficking and anchoring complexes revealed by proteomic analysis of inward rectifier potassium channel (Kir2.x)-associated proteins. J Biol Chem. 2004; 279(21):22331–22346. [PubMed: 15024025]

Leuchowius KJ, Weibrecht I, Soderberg O. In situ proximity ligation assay for microscopy and flow cytometry. Current protocols in cytometry / editorial board, J Paul Robinson, managing editor [et al] Chapter. 2011; 9 Unit 9 36.

Li H, Chuang AZ, O'Brien J. Photoreceptor coupling is controlled by connexin 35 phosphorylation in zebrafish retina. J Neurosci. 2009; 29(48):15178–15186. [PubMed: 19955370]

Li H, Zhang Z, Blackburn MR, Wang SW, Ribelayga CP, O'Brien J. Adenosine and Dopamine Receptors Coregulate Photoreceptor Coupling via Gap Junction Phosphorylation in Mouse Retina. J Neurosci. 2013; 33(7):3135–3150. [PubMed: 23407968]

Lin B, Masland RH, Strettoi E. Remodeling of cone photoreceptor cells after rod degeneration in rd mice. Exp Eye Res. 2009; 88(3):589–599. [PubMed: 19087876]

Liu X, Hirano AA, Sun X, Brecha NC, Barnes S. Calcium channels in rat horizontal cells regulate feedback inhibition of photoreceptors through an unconventional GABA- and pH-sensitive mechanism. J Physiol. 2013; 591(13):3309–3324. [PubMed: 23613534]

Mills SL, Massey SC. Distribution and coverage of A- and B-type horizontal cells stained with Neurobiotin in the rabbit retina. Visual Neuroscience. 1994; 11(3):549–560. [PubMed: 7518689]

Molina AJ, Verzi MP, Birnbaum AD, Yamoah EN, Hammar K, Smith PJ, Malchow RP. Neurotransmitter modulation of extracellular H+ fluxes from isolated retinal horizontal cells. J Physiol. 2004; 560(Pt 3):639–657. [PubMed: 15272044]

Morgans CW, Brandstatter JH, Kellerman J, Betz H, Wassle H. A SNARE complex containing syntaxin 3 is present in ribbon synapses of the retina. J Neurosci. 1996; 16(21):6713–6721. [PubMed: 8824312]

Murakami M, Shimoda Y, Nakatani K, Miyachi E, Watanabe S. GABA-mediated negative feedback from horizontal cells to cones in carp retina. Jpn J Physiol. 1982; 32(6):911–926. [PubMed: 7169699]

Nagura H, Ishikawa Y, Kobayashi K, Takao K, Tanaka T, Nishikawa K, Tamura H, Shiosaka S, Suzuki H, Miyakawa T, Fujiyoshi Y, Doi T. Impaired synaptic clustering of postsynaptic density proteins and altered signal transmission in hippocampal neurons, and disrupted learning behavior in PDZ1 and PDZ2 ligand binding-deficient PSD-95 knockin mice. Mol Brain. 2012; 5:43. [PubMed: 23268962]

Oliva C, Escobedo P, Astorga C, Molina C, Sierralta J. Role of the MAGUK protein family in synapse formation and function. Dev Neurobiol. 2012; 72(1):57–72. [PubMed: 21739617]

Pan F, Keung J, Kim IB, Snuggs MB, Mills SL, O'Brien J, Massey SC. Connexin 57 is expressed by the axon terminal network of B-type horizontal cells in the rabbit retina. J Comp Neurol. 2012; 520(10):2256–2274. [PubMed: 22495514]

Pan F, Massey SC. Rod and cone input to horizontal cells in the rabbit retina. J Comp Neurol. 2007; 500(5):815–831. [PubMed: 17177254]

Peng YW, Blackstone CD, Huganir RL, Yau KW. Distribution of glutamate receptor subtypes in the vertebrate retina. Neuroscience. 1995; 66(2):483–497. [PubMed: 7477889]

Prochnow N, Hoffmann S, Vroman R, Klooster J, Bunse S, Kamermans M, Dermietzel R, Zoidl G. Pannexin1 in the outer retina of the zebrafish, Danio rerio. Neuroscience. 2009; 162(4):1039–1054. [PubMed: 19409451]

Pruss H, Derst C, Lommel R, Veh RW. Differential distribution of individual subunits of strongly inwardly rectifying potassium channels (Kir2 family) in rat brain. Brain Res Mol Brain Res. 2005; 139(1):63–79. [PubMed: 15936845]

Puthussery T, Percival KA, Venkataramani S, Gayet-Primo J, Grunert U, Taylor WR. Kainate receptors mediate synaptic input to transient and sustained OFF visual pathways in primate retina. J Neurosci. 2014; 34(22):7611–7621. [PubMed: 24872565]

Schmitz F, Konigstorfer A, Sudhof TC. RIBEYE, a component of synaptic ribbons: a protein's journey through evolution provides insight into synaptic ribbon function. Neuron. 2000; 28(3):857–872. [PubMed: 11163272]

Sherry DM, Mitchell R, Standifer KM, du Plessis B. Distribution of plasma membrane-associated syntaxins 1 through 4 indicates distinct trafficking functions in the synaptic layers of the mouse retina. BMC Neurosci. 2006; 7:54. [PubMed: 16839421]

Sohl G, Joussen A, Kociok N, Willecke K. Expression of connexin genes in the human retina. BMC Ophthalmol. 2010; 10:27. [PubMed: 20979653]

Sohl G, Willecke K. An update on connexin genes and their nomenclature in mouse and man. Cell Commun Adhes. 2003; 10(4–6):173–180. [PubMed: 14681012]

Stroh S, Sonntag S, Janssen-Bienhold U, Schultz K, Cimiotti K, Weiler R, Willecke K, Dedek K. Cell-specific cre recombinase expression allows selective ablation of glutamate receptors from mouse horizontal cells. PLoS One. 2013; 8(12):e83076. [PubMed: 24349437]

Sun Z, Risner ML, van Asselt JB, Zhang DQ, Kamermans M, McMahon DG. Physiological and molecular characterization of connexin hemichannels in zebrafish retinal horizontal cells. J Neurophysiol. 2012; 107(10):2624–2632. [PubMed: 22357795]

Thoreson WB, Mangel SC. Lateral interactions in the outer retina. Prog Retin Eye Res. 2012; 31(5): 407–441. [PubMed: 22580106]

Tomita S, Nicoll RA, Bredt DS. PDZ protein interactions regulating glutamate receptor function and plasticity. J Cell Biol. 2001; 153(5):F19–F24. [PubMed: 11381098]

VanLeeuwen M, Fahrenfort I, Sjoerdsma T, Numan R, Kamermans M. Lateral gain control in the outer retina leads to potentiation of center responses of retinal neurons. J Neurosci. 2009; 29(19):6358–6366. [PubMed: 19439613]

Vardi N, Duvoisin R, Wu G, Sterling P. Localization of mGluR6 to dendrites of ON bipolar cells in primate retina. J Comp Neurol. 2000; 423(3):402–412. [PubMed: 10870081]

Verweij J, Kamermans M, Spekreijse H. Horizontal cells feed back to cones by shifting the cone calcium-current activation range. Vision Res. 1996; 36(24):3943–3953. [PubMed: 9068848]

Vessey JP, Stratis AK, Daniels BA, Da Silva N, Jonz MG, Lalonde MR, Baldridge WH, Barnes S. Proton-mediated feedback inhibition of presynaptic calcium channels at the cone photoreceptor synapse. J Neurosci. 2005; 25(16):4108–4117. [PubMed: 15843613]

Vila A, Satoh H, Rangel C, Mills SL, Hoshi H, O'Brien J, Marshak DR, Macleish PR, Marshak DW. Histamine receptors of cones and horizontal cells in Old World monkey retinas. J Comp Neurol. 2012; 520(3):528–543. [PubMed: 21800315]

Vroman R, Klaassen LJ, Howlett MH, Cenedese V, Klooster J, Sjoerdsma T, Kamermans M. Extracellular ATP hydrolysis inhibits synaptic transmission by increasing ph buffering in the synaptic cleft. PLoS Biol. 2014; 12(5):e1001864. [PubMed: 24844296]

Wang TM, Holzhausen LC, Kramer RH. Imaging an optogenetic pH sensor reveals that protons mediate lateral inhibition in the retina. Nat Neurosci. 2014; 17(2):262–268. [PubMed: 24441679]

Warren TJ, Van Hook MJ, Supuran CT, Thoreson WB. Sources of protons and a role for bicarbonate in inhibitory feedback from horizontal cells to cones in Ambystoma tigrinum retina. J Physiol. 2016

Zheng CY, Seabold GK, Horak M, Petralia RS. MAGUKs, synaptic development, and synaptic plasticity. Neuroscientist. 2011; 17(5):493–512. [PubMed: 21498811]

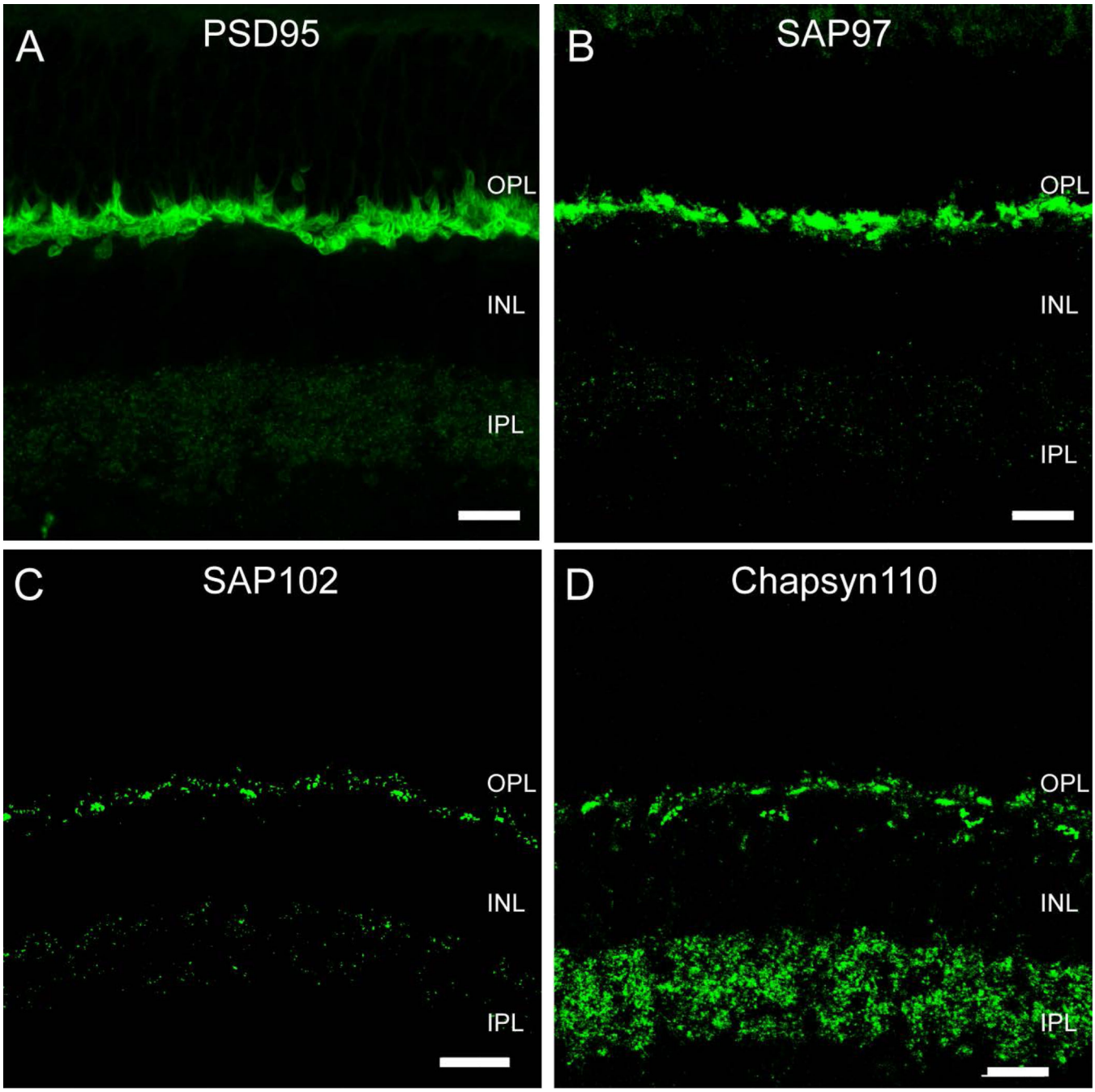

Figure 1. Membrane-Associated Guanylate Kinase (MAGUK) proteins in the rabbit retina

A, Vertical section of rabbit retina labeled for PSD95. Prominent immunoreactivity in the OPL encircled photoreceptor terminals. In the IPL immunofluorescence was found in the form of sparse, very small puncta. **B**, SAP97-IR was found in the OPL, where rod and cone photoreceptor terminals were labeled intensively. Strong labeling was concentrated in the cytoplasm of rod spherules and cone pedicles. In the IPL immunofluorescence was found in the form of sparse puncta. **C**, SAP102-IR appeared as clusters of puncta in the OPL surrounded by sparser puncta. Immunolabeling in the IPL was weak and punctate. **D**,

Chapsyn-110 IR had a similar labeling pattern as observed with SAP102 in the OPL. Chapsyn-110 immunolabeling was punctate and much stronger than the other MAGUKs in the IPL. Scale bars: 10 μm.

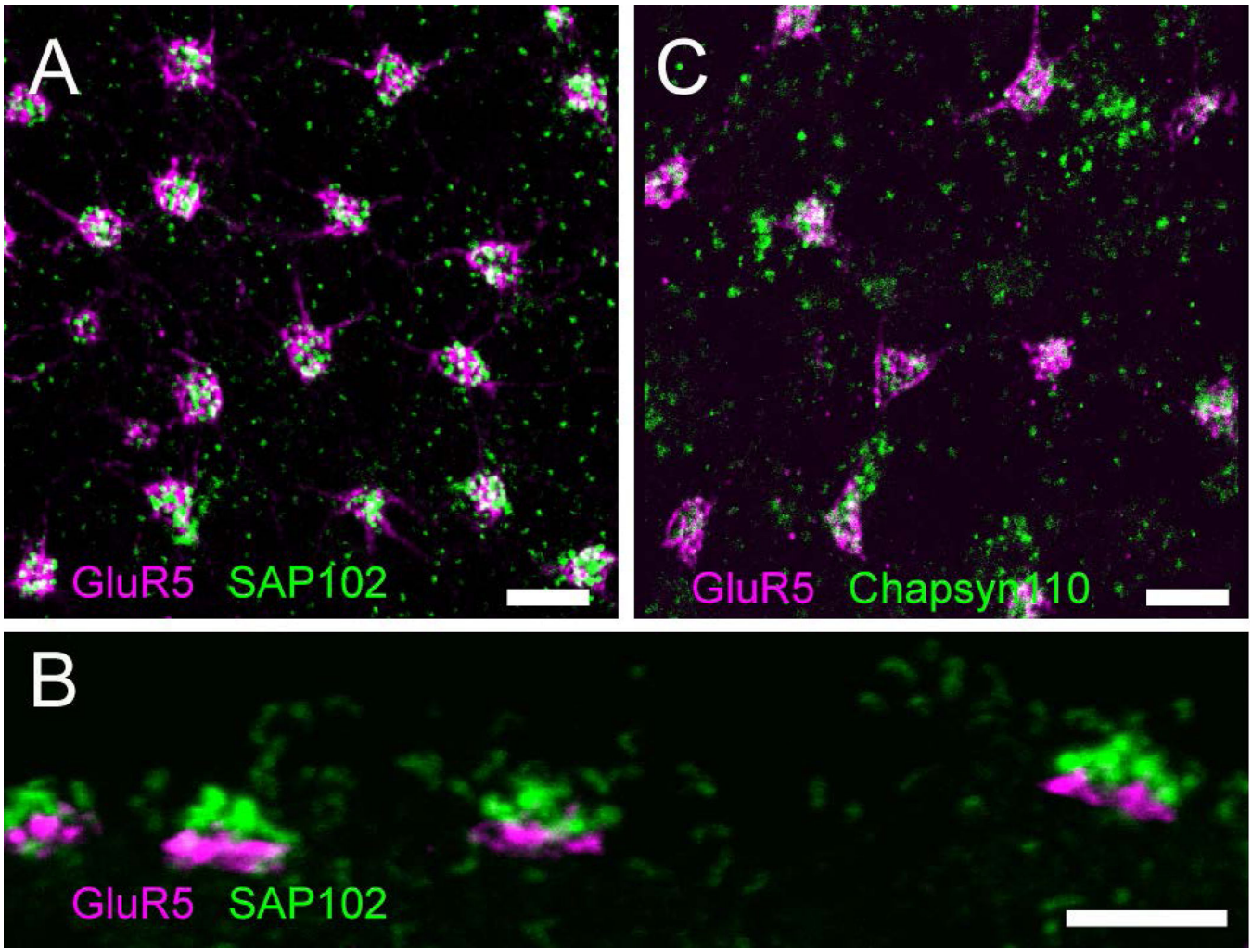

Figure 2. Clustered scaffolds are associated with cone photoreceptors

A, Wholemount immunofluorescence labeling in the OPL of SAP102 (green) and GluR5 (magenta), a marker that labels OFF bipolar cell dendrites at the base of cone pedicles. Tight clusters of SAP102 labeling were located at cone pedicles. **B**, Vertical section through the OPL with the same labeling scheme as A. SAP102 puncta were located slightly above GluR5. **C**, Chapsyn-110 (green) had similar distribution in the OPL with clusters of puncta associated with GluR5 (magenta) and distributed individual puncta. Scale bars: 5 μm.

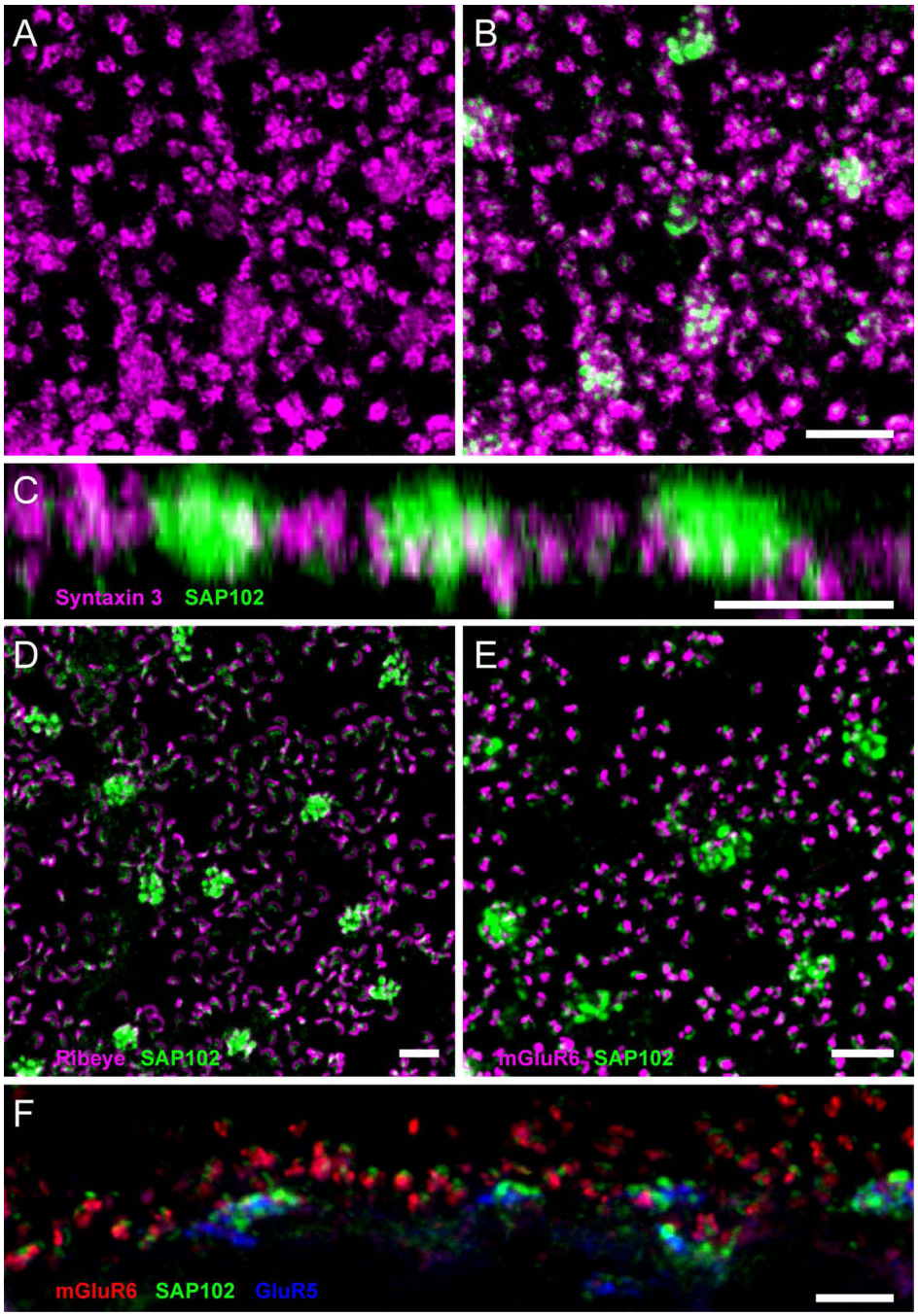

Figure 3. Association of SAP102 with synaptic elements in the OPL

A, Wholemount immunofluorescence labeling in the OPL of syntaxin 3 (magenta), revealing small clusters labeling synaptic terminals of rods, and diffuse cellular staining in cone terminals. **B**, Single optical section through the OPL double labeled for SAP102 (green) and syntaxin 3 (magenta). SAP102 labeling appears in gaps in syntaxin 3 labeling. **C**, Z-axis projection of a series of optical sections taken at 0.35 μm intervals through the OPL. SAP102 puncta in clusters were localized slightly above the cone plasma membrane labeled with syntaxin 3, suggesting that SAP102 is inside of cone pedicles and not in their plasma

membrane. One punctum was typically found per rod spherule. **D**, Wholemount immunofluorescence labeling in the OPL of SAP102 (green) and the synaptic ribbon protein ribeye (magenta). **E**, Wholemount immunofluorescence labeling in the OPL of SAP102 (green) and mGluR6 (magenta), labeling the tips of ON bipolar cell dendrites. **F**, Vertical section through the OPL with labeling of SAP102 (green), mGluR6 (red) and GluR5 (blue). The SAP102-IR puncta were always located above ON bipolar cell dendrites (mGluR6) in rods and slightly above OFF bipolar cell basal contacts (GluR5) in cones. Scale bars: 5 μm.

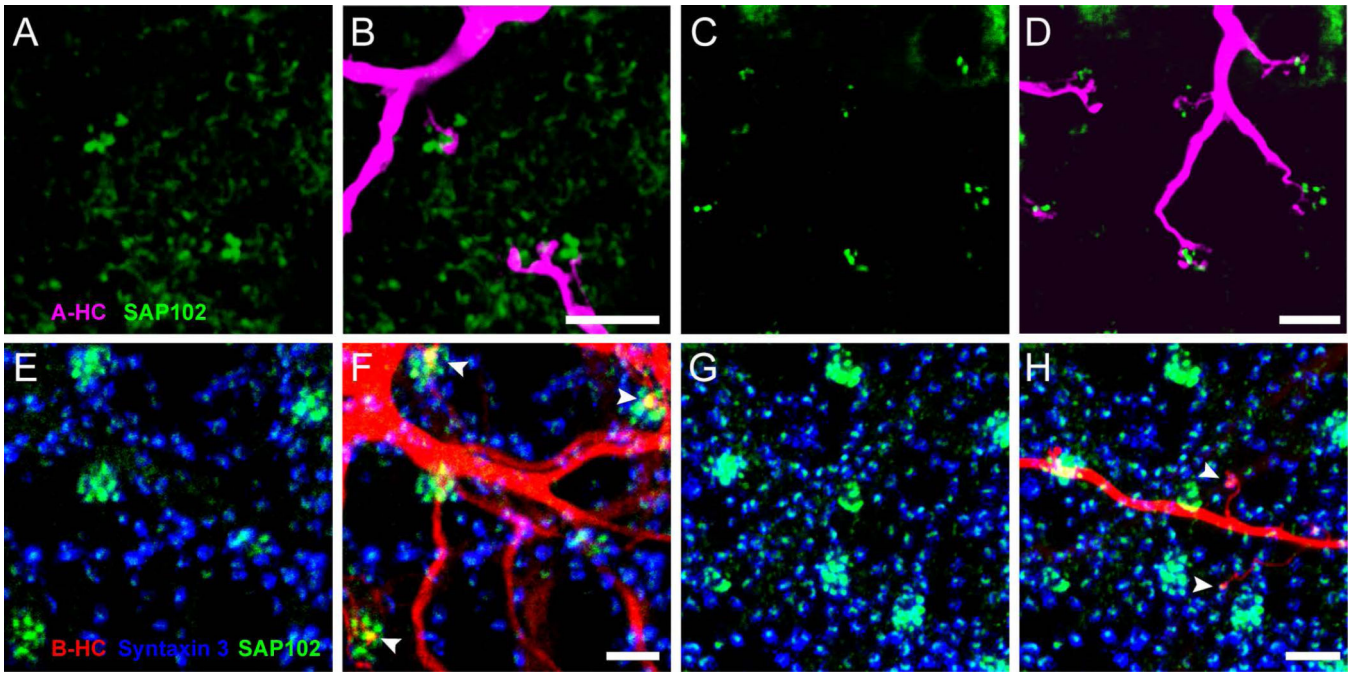

Figure 4. SAP102 is located in B-type horizontal cells

(A–D) Distribution of SAP102 (green) immunoreactivity relative to a Neurobiotin-injected A-type HC (magenta) in the OPL. **A and C**: Distribution of SAP102 immunoreactivity in the OPL. **B and D**: Stacks from 15 single optical sections at 0.25 μm increments are shown. A-type HC dendrites labeled with Neurobiotin were closely associated with clusters of SAP102 immunoreactive puncta in cones, but not co-localized. **(E–H):** Distribution of SAP102 immunoreactivity (green) relative to a Neurobiotin-injected B-type HC (red) in the OPL. **E and G**: Distribution of SAP102 immunoreactivity in the OPL. The location of photoreceptor terminals is shown with syntaxin 3 labeling (blue). Stacks from 17 single optical sections at 0.25 μm increments are shown. **F and H**, Relationships of B-type HC dendrites (**F**) and axon terminals (**H**) with SAP102. Both B-type HC dendrites (F) and axon terminals (H) colocalized with SAP102 (arrowheads) at contacts with cone terminals and rod spherules respectively. Scale bars: 5 μm.

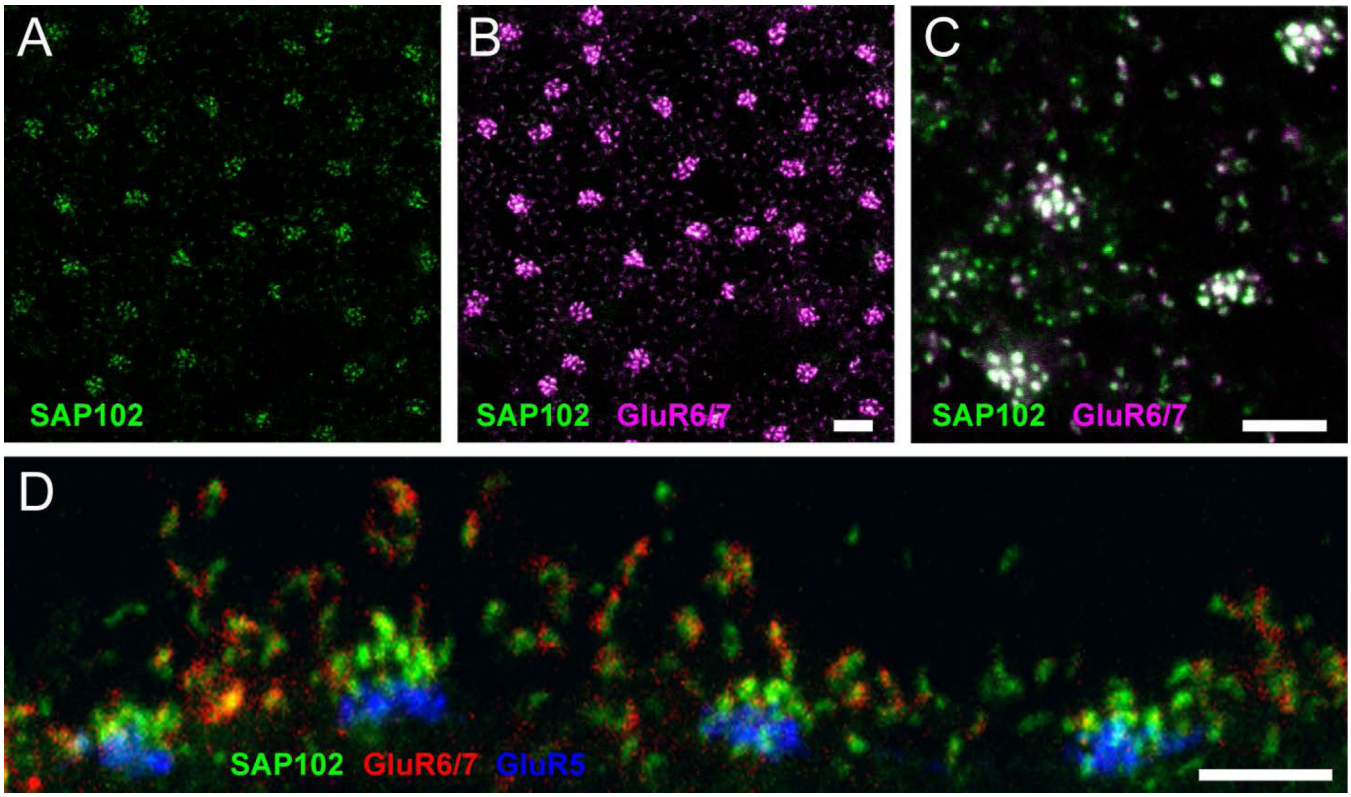

Figure 5. Association of SAP102 with kainate receptor GluR6/7

(A–C), Wholemount immunofluorescence labeling in the OPL of SAP102 (green; alone in A) and GluR6/7 (magenta). **B**, A stack from 6 single optical sections at 0.35 μm increments is shown. GluR6/7-IR appeared as discrete puncta colocalized with SAP102. **C**, Single optical section confirming that GluR6/7 colocalization with SAP102 was not due to projection of labels at different depths. **D**, Vertical section through the OPL labeled for SAP102 (green), GluR6/7 (red) and GluR5 (blue). GluR6/7 labeling was clearly colocalized with the clusters of SAP102 associated with the invaginations of rod spherules. Scale bars: 5 μm.

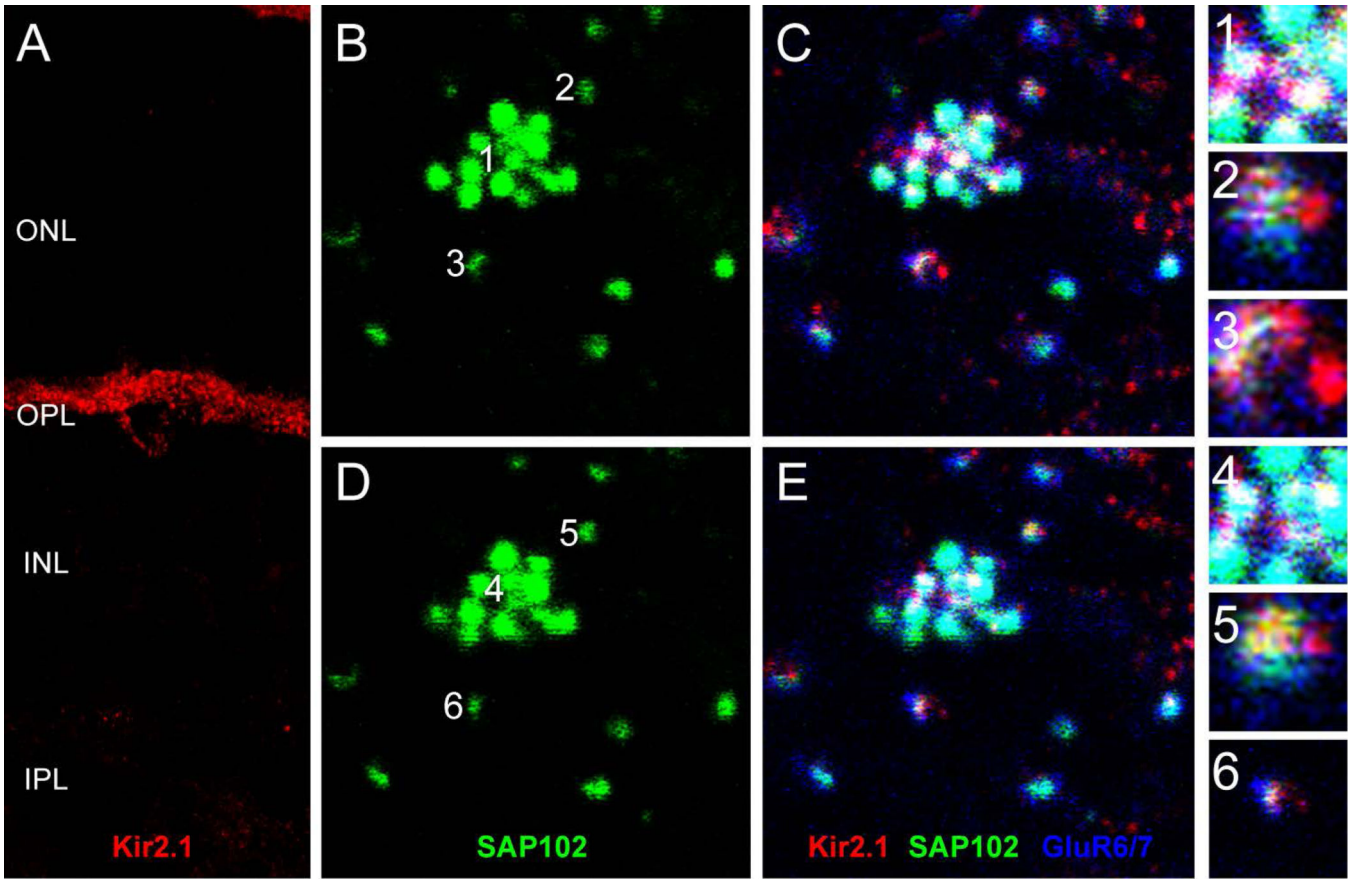

Figure 6. Association of SAP102 with inward-rectifier potassium channel Kir2.1

A, Vertical section through the retina labeled for Kir2.1. Kir2.1 exhibited a mixture of diffuse and punctate patterns in the OPL and surrounded the somas of HCs. **(B–E)**, Wholemount immunofluorescence labeling in the OPL of SAP102 (green), Kir2.1 (red) and GluR6/7 (blue) in two consecutive optical sections. B and C represent a single optical section in the lower portion of the OPL separated by 0.35 μm from a higher section in the OPL represented in D and E. **B and D**, SAP102 alone. C **and E**, Kir2.1-IR (red) was diffusely present below SAP102 clusters, but puncta were colocalized with SAP102 at the tips of HC processes. Numbers in B and D indicate individual SAP102 puncta at contacts with cone (1, 4) and rod (2–3, 5–6) terminals that are shown in the insets. Kir2.1 colocalizes with SAP102 at the level of the cones (inset 1) and at the level of the rods (insets 5 and 6). Scale bar: 5 μm.

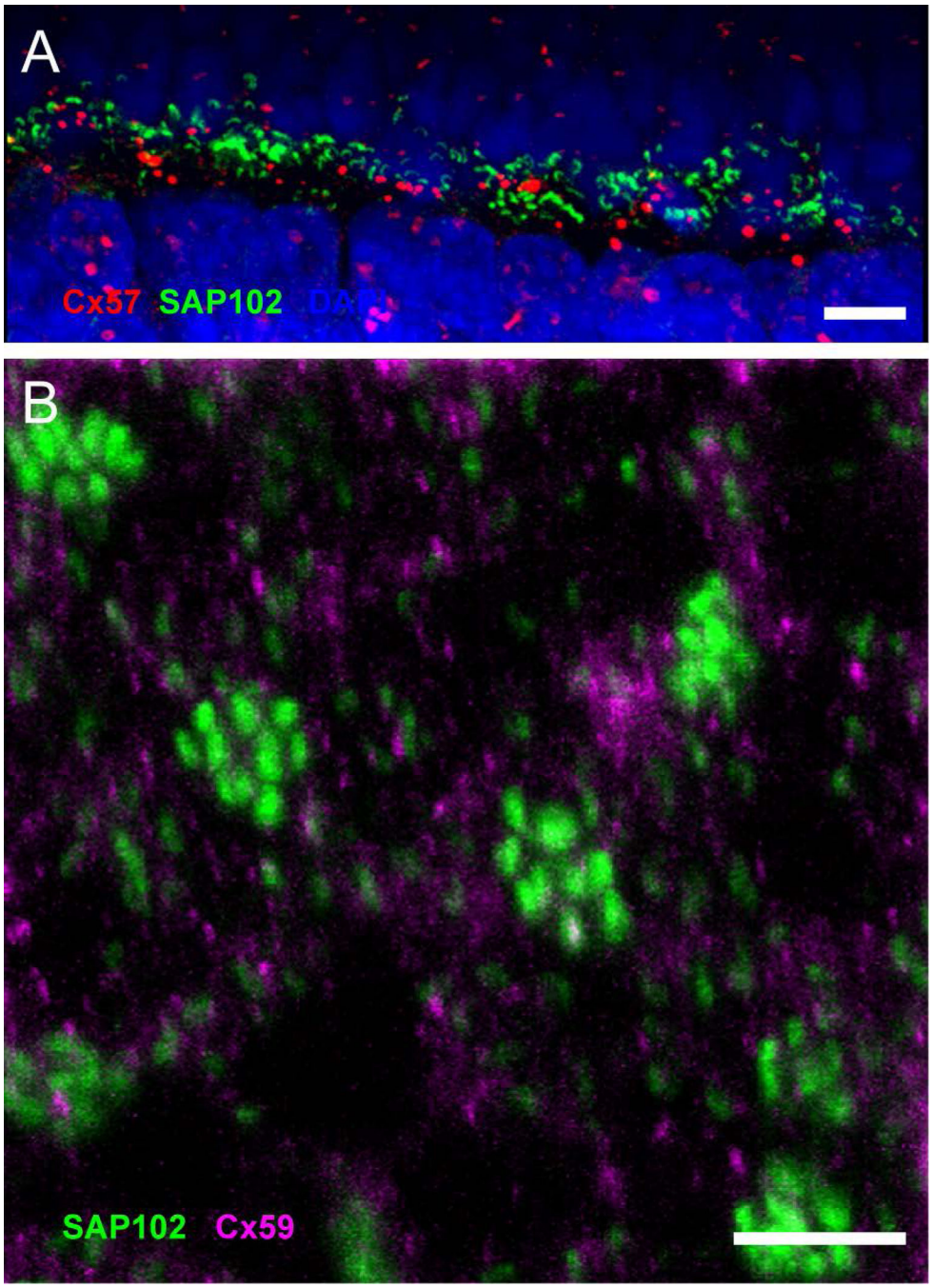

Figure 7. Connexins 57 and 59 make gap junctions in OPL but do not colocalize with SAP102

A, Vertical section through the OPL showing labeling of SAP102 (green) and Cx57 (red). Cell nuclei are labeled with DAPI (blue). No apparent relationship between the Cx57 plaques and SAP102 at either cone pedicles or rod spherules was observed. **B**, Wholemount immunofluorescence labeling in the OPL of SAP102 (green) and Cx59 (magenta). Cx59 labeling was located mostly below the SAP102-IR puncta, but was not colocalized. Scale bars: 5 μm.

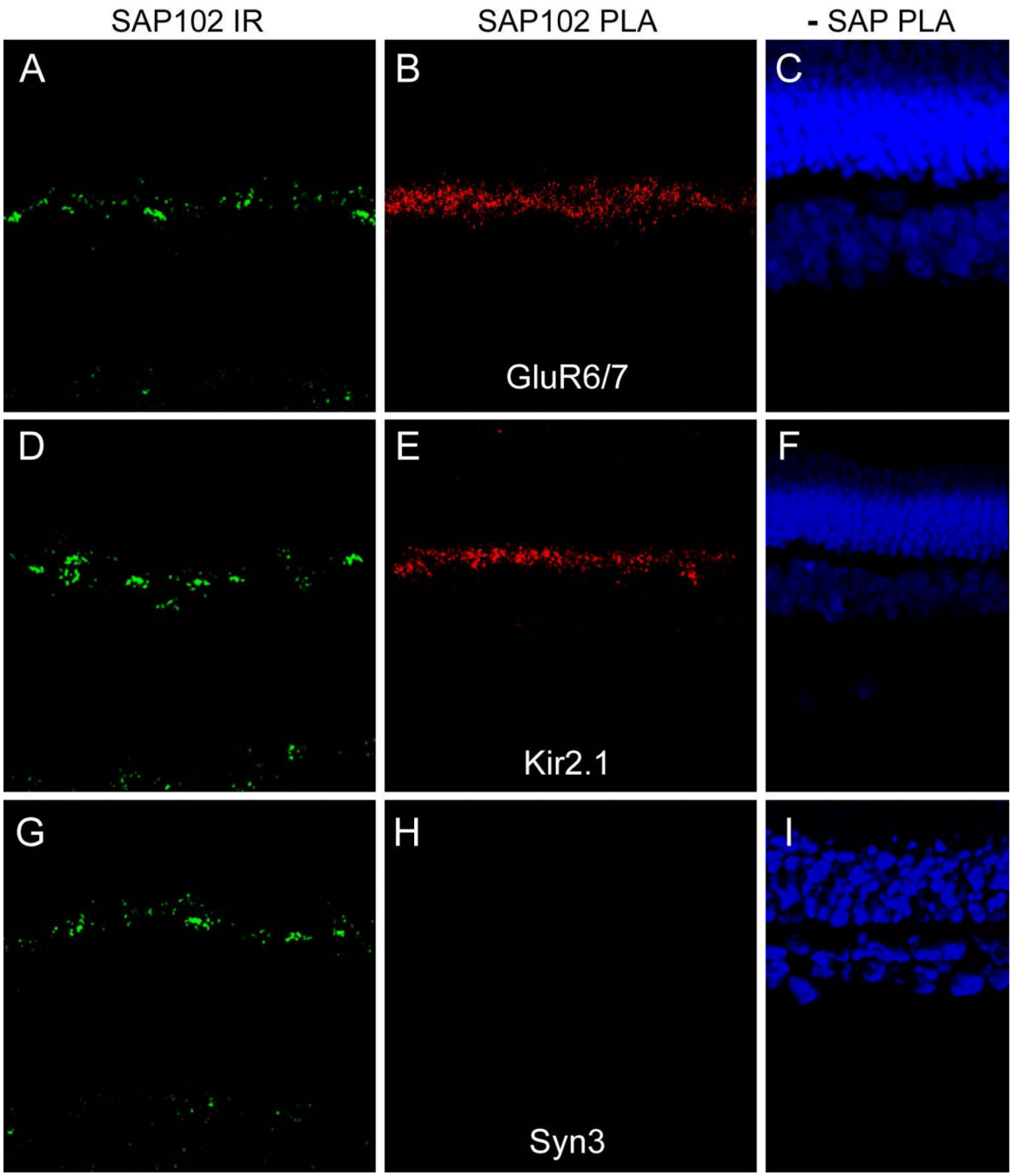

Figure 8. In situ proximity ligation assays (PLA) reveal SAP102 interactions with ion channels

SAP102 labeling (green) in a section of rabbit retina **(A)** and PLA reaction product (red) for interaction between SAP102 and GluR6/7 **(B)** in a sequential section. While SAP102 immunoreactivity occurred in both the OPL and IPL, the PLA reaction product was restricted to the OPL and appeared punctate. **C**, Negative control PLA reaction in which the SAP102 antibody was omitted; nuclei are labeled with DAPI (blue). **D–F**, PLA experiment for interaction between SAP102 and Kir2.1 using the same order and color scheme as in A–C. PLA reaction product was restricted to a narrow band of puncta in the OPL **(E)**. This

distribution was much more restricted than that of Kir2.1 in the OPL (see Fig. 6A). **G–I**, Negative control PLA experiment in which an interaction between SAP102 and syntaxin 3 was tested, using the same order and color scheme as in A-C. Although these proteins occur very close to each other on opposite sides of the photoreceptor synapses, no reaction product was detected in the OPL **(H)**

TABLE 1

Antibodies used in this study

Antibody	Host	Antigen	Source	Catalog#	Dilution	References
SAP102	Ms	Fusion protein of rat SAP102 (aa1-120)	UC Davis/NIH Neuromab, Davis, CA	75-058 RRID: AB_2261666	1:500	Haverkamp et al., 2000
PSD95	Rb	Synthetic peptide of mouse PSD95 (aa50-150)	Abcam, Cambridge, MA	ab18258 RRID: AB_444362	1:1000	Preissmann et al., 2012
PSD95	Ms	Fusion protein of human PSD95 (aa77-299)	UC Davis/NIH Neuromab, Davis, CA	75-028 RRID: AB_2292909	1:500	Puthussery et al., 2014
SAP97	Ms	Fusion protein of rat SAP97 (aa1-104)	UC Davis/NIH Neuromab, Davis, CA	75-030 RRID: AB_2091920	1:500	Koulen et al., 1999
Chapsyn 110	Ms	Fusion protein of rat Chapsyn 110 (aa1-852)	UC Davis/NIH Neuromab, Davis, CA	75-057 RRID: AB_2277296	1:500	Ogawa et al., 2008
Ribeye U2656	Rb	B domain of rat ribeye	Dr. Thomas Südhof, Stanford U. School of Medicine, CA	N/A RRID: AB_2315280	1:1000	Schmitz et al., 2000
Syntaxin 3	Rb	Residues 2–264 of mouse syntaxin 3B fused to Glutathione S-transferase	Dr. Roger Janz, U. of Texas Medical School, Houston, TX	N/A RRID: AB_2315430	1:500	Sherry et al., 2006
mGluR6	Rb	C-terminus of human mGluR6 (aa 401–419) coupled to Keyhole Limpet hemocyanin (KATSTVAAPPKGEDAEAHK)	Dr. Noga Vardi, U. Pennsylvania, Philadelphia, PA	N/A RRID: AB_2314792	1:500	Vardi et al., 2000
GluR6/7	Rb	Rat GluR6 (aa894-908) coupled to KLH (HTFNDRRLPGKETMA)	Millipore, Temecula, CA	04–921 RRID: AB_1587072	1:200	Darstein et al., 2003
GluR5	Gt	C-terminus peptide of human GluR-5 (aa 900-918) (MQFNNNYIFSIFIILH)	Santa Cruz Biotechnology, Dallas, TX	sc-7616 RRID: AB_641048	1:500	Pan et al., 2007
Kir2.1	Rb	Peptide from human Kir2.1 (aa392-410) (NGVPESTSTDTPPDIDLHN)	Millipore, Temecula, CA	AB5374 RRID: AB_91818	1:400	Giovannardi et al., 2002
Pannexin 2	Rb	Synthetic peptide derived from C-terminus of mouse Pannexin 2	ThermoFisher, Waltham, MA	42–2800 RRID: AB_2533518	1:200	

Antibody	Host	Antigen	Source	Catalog#	Dilution	References
		(SDMGDLLSIPPPQQILIATFEEPRTVVSTVEF)				
Cx57	Rb	Synthetic peptide derived from mouse Cx57 (aa 434–446) (SRLMSEKGQRHSD)	Invitrogen, Camarillo, CA	40–4800 RRID: AB_2314266	1:100	Ciolofan et al., 2007
Cx59	Rb	Synthetic peptide derived from C-terminus of human Cx59 (aa486-501) (EPGLVRPCNNPVCPPN)	Dr. Stephen Massey, U. of Texas Medical School, Houston, TX	N/A	1:100	